

RESEARCH ARTICLE

OPEN ACCESS

A refined energy-based model for friction stir processing of Al-Zn-Mg alloy

P. K. Mandal

Department of Metallurgy, Amal Jyothi College of Engineering, Kanjirapally, Kerala-686518, INDIA

Abstract

Friction stir processing (FSP) is a promising solid state surface modification technique. Also, considered as an innovative technique that the FSP was employed to modify the surface layer of aluminium alloy. The FSP passes of only two passes were applied on aluminium alloy samples. A rotating tool with a pin and shoulder is inserted into a single piece of material and results in significant microstructural changes in the processed zone, due to intense plastic deformation. It has been proved to be an effective way to refine the microstructure of aluminium alloys, and thereby improve the mechanical properties. In procedural phenomenon there are different parameters adjustment have been worked out to refine microstructure and several properties characterised to TEM, SEM, FESEM and mechanical properties. In this study, a refined energy based model that estimates the energy generated due to friction and plastic deformation is presented with the help of experimental and theoretical results available in many literatures. The model is applied to 7xxx series of aluminium alloys.

Keywords: FSP, solid-state process, processed zone, energy generation, 7xxx series.

I. Introduction

Age-hardening is the prime criteria in 7xxx series of Al alloy. It has several technological importances likely to as high strength light metal with various precipitation phases terminated from the supersaturated sold solution. There is an inseparable relationship between their improved combination of mechanical properties and the large number of fine precipitates formed during artificial ageing. The alloy composition, artificial ageing temperature and thermal history (solution treatment, quenching in water, natural ageing) are the main parameters influencing the age hardening response [1-5]. Generally, age hardening response is the increase in yield strength during artificial ageing than natural aged condition. A high yield strength implies a high resistance to dislocation motion [6]. It is also well known that adding minor scandium in aluminium alloy can refine grains and increase tensile strength, which attributed to the presence of coherent, L1₂-ordered Al₃Sc particles. It can substantially inhibit recrystallization and pin subgrain boundaries and dislocations [7-11]. By adapting the concepts of friction stir welding (FSW), a new processing technique, friction stir processing (FSP), has been recently developed. The basic concept of FSP is remarkably simple. A rotating tool with a pin and shoulder is inserted into a single piece of material and results in significant microstructural changes in the processed zone, due to intense plastic deformation at elevated temperature resulting in significant grain refinement [12-15]. Therefore, FSP has been proved to be an effective way to refine the microstructure of aluminium alloys, and thereby improve the

mechanical properties. The microstructure and properties of the modified layer depend on the amount of fractional heat generated by processing. Actually, heat is generated due to plastic deformation of the workpiece and the effect of the friction between the surfaces of the tool and the workpiece. The process is carried out in solid state at low temperature, typically around 0.6 to 0.7 of the aluminium alloy fusion temperature. The processed zone is deformed and under the thermal effect recovers and recrystallizes, forming a defect-free recrystallized fine grain microstructure. During experimental FSP, it is seen that in aluminium alloy the action of tool produces different microstructurally distinct regions; the stir zone (SZ), the thermomechanically affected zone (TMAZ) and the heat affected zone (HAZ). The stir zone is in centre of FSP and has undergone the most severe plastic deformation during processing. The stir zone grains suggest effective strains together with a microstructural evolution that occurs by a combination of hot working and a dynamic recovery or recrystallization. The temperature reached in the stir zone is known as being situated in the range of 480 °C [C.B. Fuller et al., 2010; at 640 rpm, 160 mm/min] for the aluminium alloy. The authors like Heurtier et al. and [2006] and Hamilton et al. [2008] have been proposed energy based model for the FSW during their works [16]. In fact, the energy due to plastic deformation and friction of the shoulder with the surface of the workpiece are related and competing each other. As the heat generated by the shoulder is low, the flow stress is higher and hence the resulting plastic deformation energy increases. On

the other hand, as the heat generated by the shoulder is high, the flow stress reduces and as a result the plastic strain contribution decreases. As per Khandkar's torque-based model for which the total torque is the sum of torque contributions from the tool shoulder against the workpiece, the bottom of the tool pin against thickness material and the pin surface against thickness material [17]. There are several characterizations have been done likely to FESEM (field emission scanning electron microscopy), SEM (scanning electron microscopy) and age hardening phenomena through Vicker's hardness testing. The aim of this study is to investigate the effects of double FSP passes on microstructural and mechanical properties of aluminium alloy. Besides, the effects of the plastic deformation as well as heat energy generation as compared to the theoretical and experimental results available in many literatures. In this work, heat is modelled to be generated by the friction of the shoulder and plastic deformation.

II. Experimental procedure

The research was conducted on cast plate as well as different heat treated plates of 7xxx series of aluminium alloy with the dimension as $150 \times 90 \times 8$ mm³, and the chemical composition is presented in Table-1. Standard metallographic procedures were followed for the macro and microstructural analysis. A modified Keller's reagent was used for etching of metallographic samples. The age hardening characteristics have been identified through Vicker's hardness measurements at 10 kg. load with 15 min dwell time at different time intervals at 120, 140, 180 °C temperatures, respectively. Obviously, an as-cast sample first solution treated from 465 °C for 1h then immediately water quenching (i.e., T₄ heat treatment), then maintained above artificial ageing

temperatures (i.e., T₆ heat treatment) and performed hardness sequentially upto 16 h ageing time. The cast plates were subjected to double FSP passes along the clockwise direction with predetermined rotational speed and traverse speed. The FSP was conducted on the base of a conventional vertical milling machine. The machine was well equipped with appropriate devices to collection data during working period. The materials for tensile specimens were produced (i.e., pick up along the stir zone) with tool parameters of 720 rpm (tool rotational speed) and 80 mm/min (plate travel speed) from the different heat treated conditions (in Fig.-1.a). Used tool dimensions (shoulder dia. 25 mm, shoulder height 20 mm, pin root dia. 6 mm, pin tip dia. 3 mm, and pin height 3.5 mm) were selected during experimental FSP. Similarly, the FSP tool geometry has been referred as per Hamilton et al. energy model as shown in Fig.-1(b). It is well known that the material is transported from advancing side (A) to the retreating side (R) during rotational phenomena. The plasticized material may travel many cycles around the tool before being deposited. Microstructural evolution was studied using scanning electron microscopy (SEM) and field emission scanning electron microscopy (FESEM) and the resultant mechanical properties were examined with microhardness measurements and tensile tests. Similarly, transmission electron microscopy (TEM) and X-ray diffraction (XRD) methods characterization were examined for materials intuitive precipitation phenomena. The tensile test was conducted in Instron (universal testing machine) UTM(25 KN, H25 K-S, UK). The tensile samples (flat shape sample dimensions (mm): full length 58, gauge length 26, width 4) had collected from stir zone, and tested with cross head speed 1 mm/min at room temperature.

Table-1: Chemical composition analyzed by ICP-AES (in wt%).

Alloy no.	Zn	Mg	Sc	Si	Fe	Al	Zn+Mg	Zn/Mg
1	8.24	5.67	0.87	0.88	0.42	Bal.	13.91	1.45

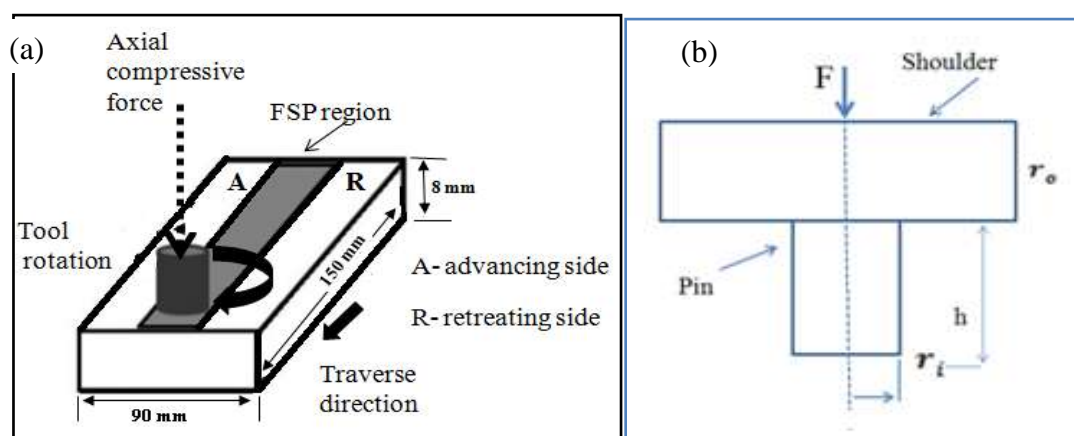


Fig.-1: (a) Schematic illustration of the friction stir processing (FSP) set-up; (b) Geometry of the FSP tool.

Table-2: Processing parameters of FSP.

FSP parameters (experiment performed through double passes)			
Tool rotation speed ω (rpm)	Work piece travel speed v_o (mm/min)	Axial compressive force F (KN)	Pin angle (°)
720	80	15	2.5

III. Results and discussion

The Al-Zn-Mg alloy is age hardening aluminium alloy. There are several phases transitions have been occurred during ageing heat treatment. The GP zones (GP I and GP II) and η are the phases that contribute to the precipitation hardening of this alloy in the under-ageing and peak-ageing conditions, while η forms during over-ageing conditions. Moreover, Sc addition in aluminium alloy consists of a spatial distribution of Al_3Sc particles. These small coherent particles with nano size were distributed homogeneously throughout the grains. Also, ample interaction between a matrix dislocation and an Al_3Sc precipitates at 400°C [18]. In Fig.-2 shows the of hardness measurements, with the error bars indicating the deviations of individual measurements. In fact, the hardness-ageing curve can be roughly divided into three regions: region I (i.e., called under-aged) with a gradual increase in harness for all ageing curves; region II (i.e., called peak-aged) with peak hardness accompanied by slight hardness decreases over a long time ageing duration; region III (i.e., called over-aged) with a further hardness decreases. In present three ageing curves have shown gradually hardness diminish due to growth of the η ($MgZn_2$) precursor particles may lead to loss of the lattice match or coherency between the matrix and the particles [19,1]. When the ageing temperature is higher the peak formation earlier than at lower ageing temperatures. On the other hand, Sc additions in aluminium alloy ageing peak formation accelerate with high value but coarsening effect one more adversely phenomena during ageing. Hardening effect of Sc useful upto 0.6 wt% beyond this coarsening effect dominates in our experimental observation and many literature references. During ageing, Al_3Sc particle coherency is maintained until a critical size is reached. Above that, heterogeneous precipitation occurs indicated by the formation of the new nuclei on dislocations and grain boundaries. As mention in literature, introduction of dislocation networks to the Al/Al_3Sc interface is most possibly related to coherency loss, low elastic strain energy

caused by the reduction in the lattice misfit [20, 8]. At 120 °C ageing shows higher hardening response in among three ageing temperatures. Stability of GP zones with high Sc content Al_3Sc particles can be claimed higher hardness value. Also, many literatures supported at this temperature GP formation and acceleration by Sc added Al-Zn-Mg alloy. At 140 °C ageing shows moderate hardening response although this temperature regime specially meant for metastable η phase formation region. But due to higher Sc contents hardening effect diminish although uniformly decrease hardness with increasing ageing time. At 180 °C ageing shows lowest hardening effect among three studied ageing temperatures. In this temperature regime hardening effect arrives earlier but coherency loss at faster rate due to higher Sc contents mostly dominate factor. On the other hand, due to higher Sc contents in aluminium alloy suppress the inherently hardening effect. In Fig.-3 shows FESEM with EDS analysis in cast aluminium alloy. The EDS analysis revealed grain boundary segregation with impurity elements and grain boundaries broaden prominent in cast aluminium alloy although Sc transition elements eliminate grain boundary segregation but probably high contents this effect decline also EDS result shows Sc-2.71%, Si-1.30%, and Fe-0.91%, respectively. Recently, a derivative from FSW, the so called friction stir processing – FSP was proved as being useful for inducing directed, localized, and controlled materials properties in any arbitrary location of components. The microstructure of the processed layer is complex and highly dependent on the position within the processed zone. This is due to the large local variations in the plastic flow, and to the thermal history resulted from the material interaction with the processing tool. In FSW/FSP, the processing technique called ‘cold working’ does not generate the melting of the nugget or stir zone. The microstructure in stir zone is characterized by refined grains in a discrete series of bands and some precipitates mainly distributed in the matrix with subgrain boundaries formation.

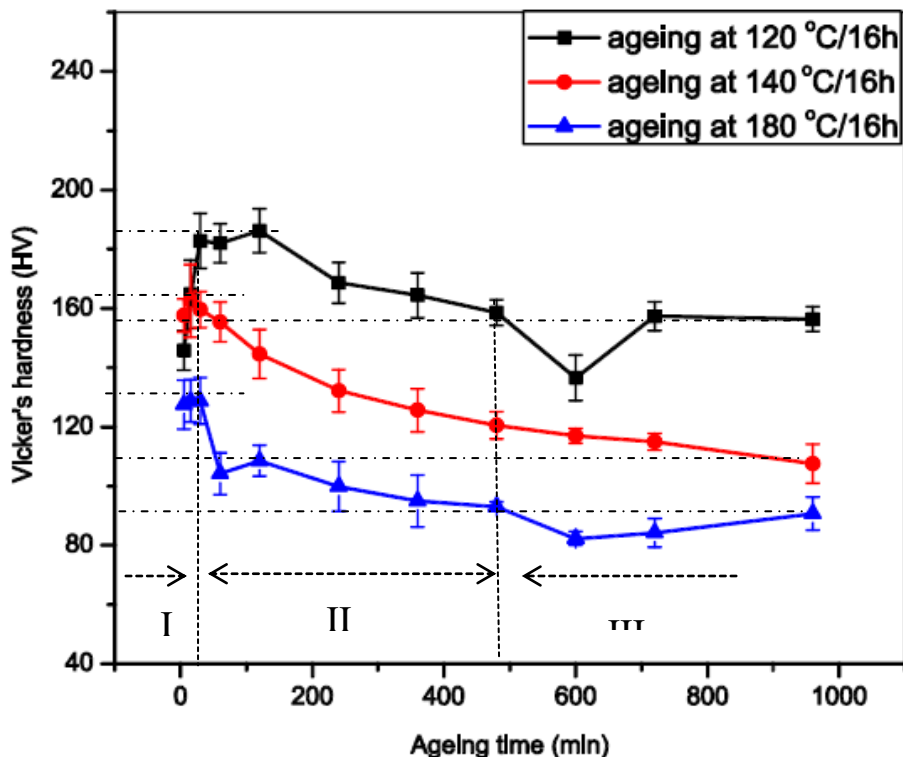


Fig.-2: The hardness-time curves plotted for a studied alloy aged at different temperatures.

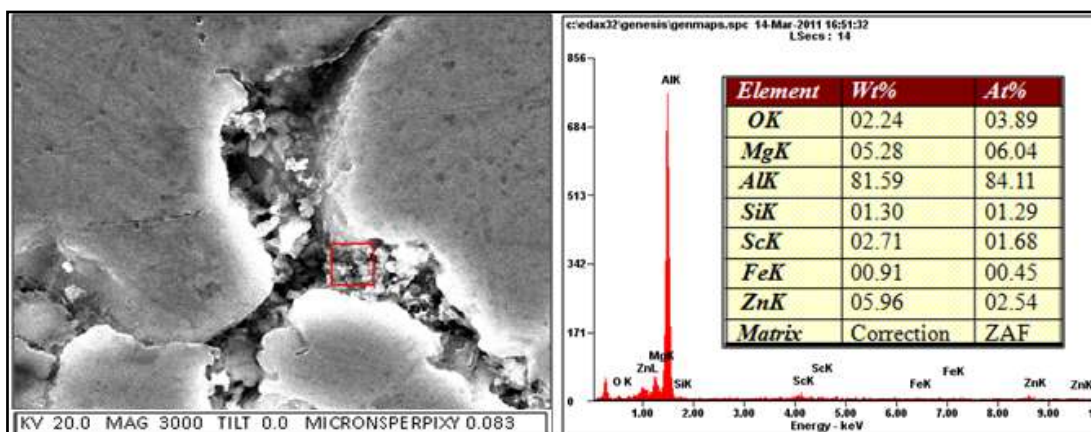


Fig.-3: FESEM with EDS analysis(as-cast condition) of studied alloy.

The stir zone grains suggest effective strains together with a microstructural evolution that occurs by a combination of hot working and a dynamic recovery or recrystallization. It is likely that sometimes low hardness in the stir zone can be attributed to dissolution of the precipitate during FSP. Generally, the hardness depends on the precipitate distribution rather than grain size. The thermo-mechanically affected zone adjacent to the nugget or stir zone is the region where the metal is plastically deformed as well as heated to a temperature, which is not sufficient to cause recrystallization. Distinct precipitates and coarsened grains are observed in HAZ regions, where the grains are severely

coarsened by FSP. There are several assumptions have been taken as per Hamilton et al. and Heurtier et al. [2006] that the heat generated due to friction of the pin shoulder on the workpiece surface is dominant and the heat generated due to the plastic deformation within the workpiece and the friction of the pin of the material is negligible. However, heat generated mostly from both the friction of the pin shoulder and plastic flow. It is assumed that the tool rotates with an angular speed of ω (rpm) and traversely translates along the line of processing with a speed of v_o (mm/min) and tool is acted upon by a compressive axial force F as shown in Fig.-1(b). According to Hamilton et al. energy model, since

FSP is the metal working technology adapted from FSW using the same basic principles [16]. Since, energy generated per unit length during processing as E is given by $E_f = P_f / v_o$(1), where P is the total power generated by friction. Assuming that the total torque due to friction of the pin, shoulder, and pin circumference with the work piece surfaces is T_f , the frictional power is then given by $P_f = T_f \omega$ (2), where ω is the pin angular speed. To find an expression for the total frictional torque T_f , we let $T_f = T_s + T_p$ (3), where T_s is the torque generated by the shoulder and T_p is torque generated by the pin. Assuming that a uniform shear stress τ occurs during processing, we obtain $T_f = 2\pi r_o^2 \tau (\frac{1}{3}r_o + \frac{r_i^2}{r_o^2}h)$(4). Assuming a coefficient of friction is μ , the total friction force F_f due to the compressive force F is given by $F_f = \mu F$ (5). It is noting that $\pi r_o^2 \tau$ is the total frictional force, then from equ.-(4) $T_f = 2\mu F (\frac{1}{3}r_o + \frac{r_i^2}{r_o^2}h)$(6). Now consider from equ.-(1) and (2), we obtain $E_f = T_f \omega / v_o = 2\mu F (\frac{1}{3}r_o + \frac{r_i^2}{r_o^2}h) \frac{\omega}{v_o}$(7). So, equ.-(7) defines the energy per unit length of the FSW/FSP due to friction between the tool and the workpiece. For a given tool geometry, tool speed, and workpiece material, this energy can be easily identified. As can be noted from equ.-(1), the power generated due to friction is given by $P_f = 2\mu F (\frac{1}{3}r_o + \frac{r_i^2}{r_o^2}h)\omega$(8). As Frigaard [1998] reported that the coefficient of friction (μ) between Al and mild steel should be set as the average value between 0.5 for sticky friction and 0.25 for dry sliding. However, in this study a coefficient of friction (μ) is used 0.5 (as per Hamilton et al.). The other source of heat is due to the plastic deformation within the workpiece. Provided that the plastic deformation within the workpiece is totally transformed into heat, the heat generated due to plastic deformation per unit FSP length can be expressed as follows: $E_p = \sigma \epsilon dV$(9), where σ and ϵ are the stress and strain, respectively, $dV = 2r_i h$ is the volume per unit length of the material. Since the effect of the energy due to plastic deformation is much smaller than that due to friction, a simple model was proposed as follows: $E_p = \sigma_e \epsilon_e 2r_i h$ (10), where σ_e is the equivalent (effective) stress and ϵ_e is the effective strain. Using the finite element method, Heurtier et al. [2006] found that the effective strain is around 6. The power generated due to the plastic deformation is given by $P_p = \sigma_e \epsilon_e (2r_i h) v_o$ (11). The total energy generated per unit length of the FSP is the sum of the energy generated due to friction between the tool and the workpiece and the plastic deformation within the workpiece. An empirical formula developed a proposed energy

model by Hamilton et al., $\frac{T_{max}}{T_s} = 1.56 \times 10^{-4} E_{eff} + 0.54$(12), where T_{max} is the maximum temperature generated within the FSP, T_s is the solidus temperature in Kelvin, E_{eff} is the effective energy generated per unit length of FSP in J/mm. In this study, one aluminium alloy is considered using different FSP parameters such as tool geometry and FSP speed. As per many literatures supported and Hamilton energy model we can be concluded $T_s = 636$ °C [from Al-Zn equilibrium phase diagram] and $T_{max} = 480$ °C[C.B. Fuller et al., 2010; at 640 rpm, 160 mm/min], its can put into equ.-(12) to obtained $E_{eff} = \frac{T_{max}}{T_s} (\frac{10^4}{1.56}) - 0.54$ (J/mm).....(13). Considering equ.-13, we can be obtained $E_{eff} = 5319.97$ J/mm. Consequently, as per Khandkar's torque-based model for which the total torque, T_{total} , is expressed as the sum of torque contributions from the tool shoulder against the workpiece, the bottom of the tool pin against thickness material and the pin surface against thickness material. Therefore, $T_{total} = 2\mu F (\frac{1}{3}r_o + \frac{r_i^2}{r_o^2}h)$(14), where, μ (0.5 value) is the coefficient of friction between the tool and the workpiece, F is the applied force, r_o is the radius of the tool shoulder, r_i is the radius of the pin, h is the pin height. The total energy per unit length of FSW, E_{total} is found by dividing the average power, P_{avg} by the weld velocity to yield the expression using $E_{total} = \frac{P_{avg}}{v_w} = T_{total} \frac{\omega}{v_w}$ (15), where v_w is the velocity during FSW and ω is the tool angular velocity. As per C. Hamilton et al. [2009] proposed his paper during FSW welding temperature is equal to the solidus temperature of aluminium alloy, i.e., $\frac{T_{max}}{T_s} = 1$. So, from the equ.-(13) we can easily found out $E_{eff} = 6409.72$ J/mm. for the Sc-modified Al-Zn-Mg-Cu alloy examined in this work, the model successfully predicts the maximum welding temperature and temperature distributions over the energy range investigated by C. Hamilton et al.. The model, however, shows its greatest potential at higher energy welds (i.e., $(E_{total})_{eff} > 1000$ J/mm) where heat generation due to friction dominates. At the lower energy levels (i.e., $(E_{total})_{eff} < 1000$ J/mm), the predicted temperature data in terms of magnitude and shape away from the tool shoulder, but the model under-predicts the maximum welding temperatures due to the assumptions/simplifications that were used in the calculation of the plastic energy. According to H. Lombard et al., hinted that the basic energy model based on the external FSW parameters [21, 22]. Heat input from the tool shoulder per unit length of weld (J/mm) can be estimated from torque measurements that remain reasonably constant once thermal equilibrium is reached and given by $Q = \frac{\text{Power}}{\text{Traverse speed}}$

$= \eta \frac{2\pi\omega T}{v}$(16), where Q is the heat input (J/mm), η = efficiency factor = 0.9 (for Al and Cu), ω (rpm) is the rotational speed, T (Nm) is the torque, v (mm/min) is the traverse speed. They also hinted on

heat input appears to be dominated by the traverse speed, suggesting that changes in the rotational speed are compensated by changes in the torque. In Fig.-4 shows different FSP

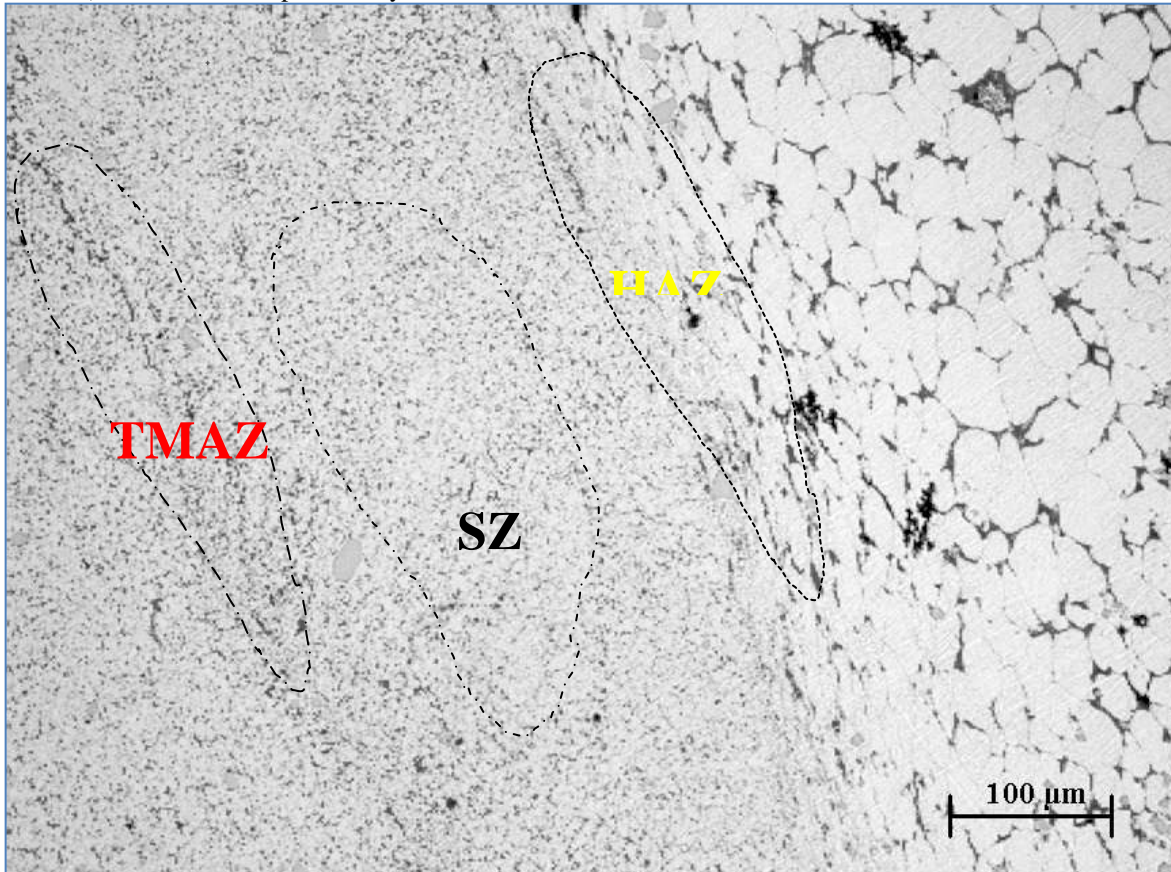


Fig.-4: The illustration of optical micrograph (at $T_4 + \text{FSP}$) of different FSP regions of studied alloy.

regions which has created during this processing just because tool shoulder with workpiece downward frictional force with predetermined tool geometry and predetermined FSP parameters, which can be created three distinct zones likely to stir zone (SZ- centre zone as equal area of pin diameter), thermo-mechanically affected zone (TMAZ- nearer to stir zone), and heat affected zone (HAZ- nearer to thermo-mechanically affected zone), also identified in specific regions in optical micrograph. As a result, stir zone is the most effective region to refine microstructure to modify material surface characteristics and enhanced mechanical properties. Hence, main aim of the investigation is to determine the relationship between parameters of the process (rotational speed, traverse speed, downward force, and type of tool design) and torque (Nm) and temperature generated in the stir zone [A.N. Solonin et al., 2010; P. Heurtier et al., 2006]. Torque, temperature and stress generated by the movement and friction of materials, decide about heat generation in the modified material and thus the changes of microstructure and consequently the

mechanical properties of material. It is evidence that the torque strongly depends on the rotational speed of the FSP tool. This is because the rotational speed stimulates the temperature in the FSP area and thus the friction coefficient decreases when temperature increases. The value of torque is influenced by rotational speed, travelling speed, downward force, design of tool, and a kind of modified material. Here, the experimental results are compared with the results obtained from the theoretical models. In Fig.-5(a-b) shows tensile fractographs at different conditions, for Fig.-5(a) has indicated ductile mode of fracture surface and microcracks are normally originated from grain boundaries (e.g. generally called intergranular fracture mode) and fine precipitates are appears mostly in grain boundary regions in between some black holes also indicate origin of fracture initiation. Similarly, in Fig.-5 (b) shows fracture surfaces are blunt due to may ageing exposed indication and overall fracture surface indicating uniformly arranged with some dip black holes observed. These black holes are possibly indication of stress centre. This studied alloy has Sc content 0.87%, which can be

deleterious effect of coarsening tendency during post ageing heat treatment. During age hardening treatment at 140 °C ageing hardness dropped marginally than at lower ageing temperature. Consequently, during tensile testing also indicated at this condition overall mechanical properties diminish. Since, aluminium alloy is prominent for age hardening ability to response natural ageing and subsequently artificial ageing tendency at elevated temperatures. The age hardening kinetics can be revealed through tensile testing measurement, also depend on chemical composition, heat treatment conditions and after all surface modification technique, so called FSP. In Table-3 shows tensile results at different FSP conditions in three stages at as-cast plus FSP condition exhibited higher tensile properties due to cast condition with FSP hardening phases (η -Mg₂Zn) are homogeneously distributed with fine grains cause dynamic recrystallization and presence of coherent Al₃Sc particles. But hardness value (105.8HV) indicated lowest due to higher

ductility. Consequently, T₄ heat treatment plus FSP condition tensile properties are slightly dropped due to specific solution treatment the hardening phases are dissolution occurred, possibly. One more possibility may happen for solution treatment Al₃Sc particles remain in solution, particles have not taken part hardening activity as like during ageing phenomena hardening stimulated with time. But hardness value (153.6HV) is highest due to higher Sc contents. After T₄ plus FSP with post ageing treatment tensile properties dropped drastically because material become overaged with predominantly incoherent equilibrium (η) phases, particle coarsening particularly at grain boundary regions. Other hand, at FSP with post-heating specimen often exposed faster precipitates nucleation (i.e., depends nature of material, time, and temperature) with facilities of high angle grain boundaries are main factors. Similarly, hardness value (128.2HV) dropped drastically due to higher Sc contents to faster precipitates coarsening effect.

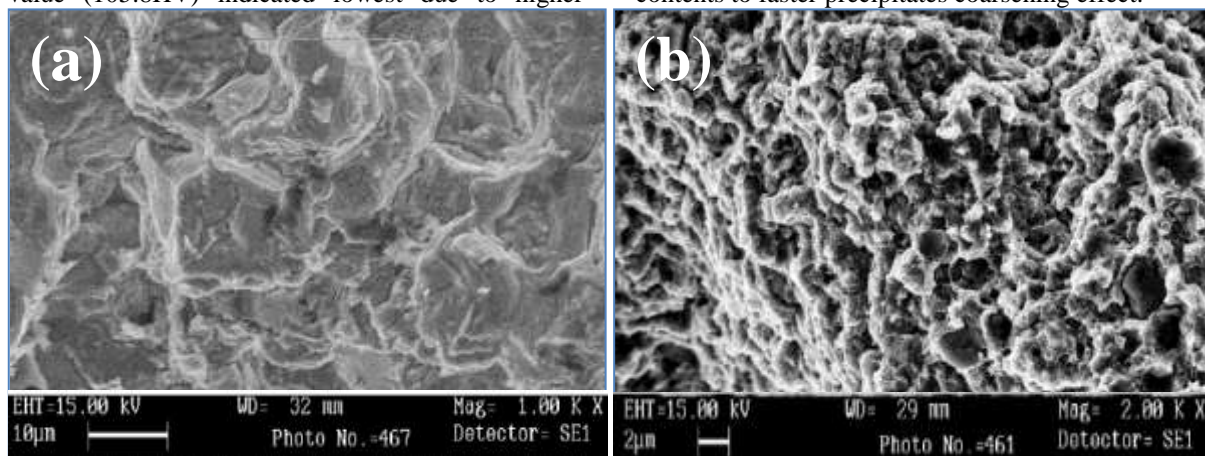


Fig.-5: The tensile fractographs of studied alloy (a) at T₄+FSP; (b) at T₄+FSP+Ageing at 140 °C/2h.

Table-3: Results of tensile properties are tabulated through FSP direction of studies alloy.

FSP by double passes at different conditions	Tensile properties			
	$\sigma_{0.2}$ (MPa)	σ_u (MPa)	δ (%)	VHN _(10kg.)
AC + FSP	99.4	207.8	5.7	105.8
T ₄ + FSP	98.9	197.6	4.3	153.6
T ₄ + FSP + Aged at 140 °C /2h	79.2	168.5	5.2	128.2

Note: AC= as-cast; T₄ = solutionized at 465 °C/1 h then WQ; yield strength denoted at 0.2% offset from stress-strain curve. Hardness (at average six values) taken along the stir zone.

IV. Conclusions

1. The Al-Zn-Mg alloy is the best age hardening performer in all aluminum series.
2. Based on experimental results Sc is best hardener in cast aluminum alloy within the limit 0.25-0.60 wt%.
3. Adding minor scandium in aluminium alloy can refine grains and increase tensile strength, which attributed to the presence of coherent, L₁₂-ordered Al₃Sc particles. It can substantially

- inhibit recrystallization and pin subgrain boundaries and dislocations.
4. At higher Sc contents diminish age hardening effect and deteriorate overall mechanical properties.
5. The friction stir processing (FSP) originates from the technology of friction stir welding (FSW), yet in comparison with this method, the phenomena taking place in the interface between the stirring area and the workpiece will have a

- decisive effect on the functional properties of a surface layer obtained through this process.
6. The friction stir processing (FSP) is a promising solid state surface modification technique. Also, considered as an innovative technique that the FSP was employed to modify the surface layer of aluminium alloy. The FSP process addresses the industry as surface repairing technique in case of different types of flows.
7. The proof stress and tensile stress dropped marginally due to elimination of residual stresses, dissolution of precipitates (η -MgZn₂) and grains coarsening are main reasons.
8. The goal of presented work is to estimate the relationship between FSP parameters such as rotational and travelling speed, downward force, torque, temperature.
9. There are several theoretical energy-based models explained for better coincidence with present experimental data. According to Heurtier et al. and Hamilton et al. a simply energy-based model for the FSW/FSP is proposed. The model aims at estimating the heat generated due to plastic deformation within the workpieces and friction between the tool surfaces and the workpieces. A comparison between the estimated heat energy and its corresponding maximum temperature obtained using the proposed model and the experimental result shows a good agreement.
10. Here, we have discussed Khandkar's torque-based model that is good agreement with heat energy generated is a function of applied force, coefficient of friction between the tool and the workpiece, tool dimensions, and FSW/FSP parameters. As per Khandkar's torque-based model and Hamilton energy-based model's correlation has been found out effective energy value (E_{eff}) during our experiment work. The numerical value is $E_{eff} = 6409.72 \text{ J/mm}$. This is good agreement with Khandkar's torque-based model value. Also, from our experimental data obtained value is $E_{eff} = 5319.97 \text{ J/mm}$. As per H. Lombard et al. explained basic energy based model, also explained amount of heat generation depends on process parameters.
- [5] H. Loffler et al., Journal of Materials Science 18 (1983) 2215-2240.
- [6] E. Hornbogen et al., Acta Metall. Mater. Vol. 41, No. 1, pp. 1-16, 1993.
- [7] B. Li et al., Journal of Alloys and Compounds 584 (2014) 406-416.
- [8] D. Tsivoulas et al., Materials Science Forum, Vols. 519-521 (2006) pp. 473-478.
- [9] Z. Ahmad, Journal of Materials, Feb.2003, pp. 35-39.
- [10] A.L. Berezina et al., Materials Science Forum, Vols. 396-402 (2002) pp. 741-746.
- [11] Y. Deng et al., Journal of Alloys and Compounds 530(2012) 71-80.
- [12] C.G. Rhodes et al., Scripta Materialia 48 (2003) 1451-1455.
- [13] S. Soleymani et al., Journal of Surface Engineering Materials and Advanced Technology, 2011, 1, 95-100.
- [14] C.B. Fuller et al., Materials Science and Engineering A 527 (2010) 2233-2240.
- [15] J-Q. Su et al., Scripta Materialia 52 (2005) 135-140.
- [16] S. A. Emam et al., World Academy of Science, Engineering and Technology 53, 2009, pp. 1016-1022.
- [17] C. Hamilton et al., International Journal of Machine Tools & Manufacturing 49 (2009) 230-238.
- [18] B.G. Clark et al., Journal of Materials Research, Vol. 20, No. 7, July 2005, pp. 1792-1801.
- [19] W. Feng et al., Rare Metals, Vol. 26, No. 2, Apr. 2007, pp. 163-168.
- [20] J. Royset et al., International Materials Reviews, 2005, Vol. 50, No. 1, 19-44.
- [21] M.S. Weglowski et al., Key Engineering Materials, Vols. 554-557 (2013) pp. 1787-1792.
- [22] H. Lombard et al., Materials Science and Engineering A 501 (2009) 119-124.

References

- [1] J.Z. Liu et al., Scripta Materialia 63 (2010) 1061-1064.
- [2] S. Ahmadi et al., Journal of Alloys and Compounds 484 (2009) 90-94.
- [3] J.K. Park et al., Metallurgical Transactions A, Vol. 14A, Oct. 1983, 1957-1965.
- [4] W.J. Poole et al., Metallurgical and Materials Transactions A, Vol. 31A, Sept. 2000, 2327-2338.